THE ASTROPHYSICAL JOURNAL, 416:587–600, 1993 October 20

DIFFUSE GAMMA-RAY EMISSION IN THE GALACTIC PLANE FROM COSMIC-RAY, MATTER, AND PHOTON INTERACTIONS

D. L. BERTSCH,[1] T. M. DAME,[2] C. E. FICHTEL,[1] S. D. HUNTER,[1] P. SREEKUMAR,[1,4]
J. G. STACY,[3] AND P. THADDEUS[2]

Received 1992 September 28; accepted 1993 April 16

ABSTRACT

On the basis of the spatial distribution, intensity, and energy spectrum, the diffuse Galactic high-energy gamma radiation is believed to be the result of cosmic-ray interactions with matter, and to a lesser extent photons. This paper describes a model calculation of diffuse gamma-ray emission based on these interactions. Recent radio observations of the main interstellar components of matter on a scale of 0°.5 are used for the entire region within 10° of the Galactic plane. A three-dimensional spatial model of the Galaxy is used to compute the emission from each volume element based on the matter, cosmic ray, and photon densities using well know interaction processes. Provisions are incorporated to account for the near-far ambiguity in determining the distance of matter in the inner Galaxy that results from Galactic rotation velocity-distance relationship. Cosmic-ray densities are modeled from the matter distribution using dynamical balance arguments, and they are expressed as a coupling scale length. This length, together with the normalization factor used to convert the observed CO line intensity to the molecular hydrogen density, are the only two adjustable parameters in the model. This approach provides a framework for calculating the observed intensity without invoking symmetries in longitude which can dilute spatial differences related to interesting spiral arm features, and it provides for a wide range of assumptions regarding the cosmic-ray distribution to be readily tested. The calculations are compared with existing data, and the values of the parameters are given. It is expected that new results from the EGRET instrument, when used with this model, will contribute to a better understanding of the cosmic ray distribution and the relation between CO and atomic hydrogen. Both of these issues are significant for studies of the dynamics and structure of the Galaxy.

Subject headings: cosmic rays — diffuse radiation — Galaxy: structure — gamma rays: observations

1. INTRODUCTION

When the sky is surveyed in high-energy gamma rays, the most intense feature is the narrow band of emission along the Galactic plane, first seen by *OSO 3* (Kraushaar et al. 1972) and with a high altitude balloon experiment (Fichtel et al. 1972). It is particularly strong in a region about 100° wide including the Galactic center. The first results from *SAS 2* showed that the radiation was generally correlated with major large-scale features such as the molecular ring, the intense Cygnus and Vela regions, broad interarm regions, and in some cases the tangents of spiral arms. Subsequent work using the complete results from both *SAS 2* (Fichtel et al. 1975; Hartman et al. 1979) and *COS B* (Mayer-Hasselwander et al. 1980, 1982) have generally verified and extended the association of gamma-ray features with structural features of the Galaxy. For example, prominent gamma-ray maxima occur at two of the best defined spiral arm tangents, Carina at $l \approx 285°$ and Crux at $l \approx 315°$. Even at intermediate latitudes, a significant portion of the gamma radiation observed is believed to be Galactic, given its correlation with the matter and other indicators (Fichtel, Simpson, & Thompson 1978; Thompson & Fichtel 1982).

On the basis of the distribution, intensity, and energy spectrum, the diffuse gamma radiation is generally thought to have its origin in the cosmic-ray interactions with matter and to a lesser extent with photons. As a result, combined information from gamma-ray observations and those at other wavelengths, particularly radio, is expected to provide valuable evidence on the role that the cosmic rays play in the Galaxy. Another advantage to using gamma-ray and radio measurements to study the Galaxy is that unlike optical photons and X-rays, which are absorbed in a small fraction of the distance between the Sun and the Galactic center, high-energy gamma rays suffer only negligible absorption through the entire plane of the Galaxy, and although uncertainties exist concerning the radiative transfer of both the CO and 21 cm lines, they are fairly reliable gas tracers, particularly on a Galactic scale. The study of the diffuse Galactic gamma radiation may also be able to contribute to obtaining a better estimate of the ratio of the CO line emission intensity to molecular hydrogen column density and hence the mass calibration of molecular clouds since cosmic rays interact with the nuclei of both atomic and molecular hydrogen in an unbiased manner.

It is worth reviewing briefly some of this earlier work to place the model and calculations to be described here in context. Many scientists were stimulated by the *SAS 2* results (Kniffen et al. 1973; Fichtel et al. 1975; Thompson et al. 1977) that showed the clear correlation of the great majority of the diffuse high-energy gamma radiation with large-scale Galactic features. Bignami & Fichtel (1974) developed a cylindrically symmetric model involving strong coupling between the cosmic rays and the interstellar matter on the scale of Galactic arms based on considerations of Galactic dynamic balance. Bignami et al. (1975) extended this concept of matter–cosmic-ray coupling in a model with spiral structure, obtaining good agreement. Another early approach was taken by Schlickeiser & Thielheim (1974*a*, *b*) and Thielheim (1975) who also noted

[1] NASA/Goddard Space Flight Center, Greenbelt, MD 20771.
[2] Harvard-Smithsonian Center for Astrophysics, Cambridge, MA 02138.
[3] University of New Hampshire, Durham, NH 03824.
[4] Universities Space Research Association.

that the cosmic rays should be coupled to some portion of the matter through the Galactic magnetic fields. Dodds, Strong, & Wolfendale (1975) similarly concluded that an extragalactic origin of the cosmic rays was improbable owing to their distribution. Assuming a power-law dependence between the magnetic field strength and the product of the cosmic ray and matter densities, and using the spiral magnetic field model of Thielheim & Langhoff (1968), they found that reasonable agreement with the gamma-ray observations is obtained by using a third- to fourth-power dependence of this product on the magnetic field. Paul, Casse, & Cesarsky (1975) noted that similarities in the observed spatial variations of the Galactic high-energy gamma rays and 150 MHz radio emission, as well as radio observations of M31 suggest a proportionally between the cosmic-ray density, the gas density, and the square of the magnetic field strength.

Fuchs, Schlickeiser, & Thielheim (1976) used the preliminary estimates of the Galactic molecular hydrogen distribution deduced from CO line measurements of Scoville & Solomon (1975) and found that no power-law relationship between cosmic rays and gas density gave a particularly good agreement with the gamma-ray observations. In addition, the estimates of the H I gas densities that these authors used does not appear to be in agreement with more recent observations. Stecker et al. (1975) used the same CO measurements to deduce the shape of the molecular hydrogen distribution, but normalized the actual density by using infrared and X-ray absorption measurements. Puget et al. (1976) considered the effects of localized concentrations of matter in the Galaxy. They deduced that the gamma-ray distribution follows that of Population I stars and giant H II regions between 0° and 180° longitude. Using H I and CO surveys, they computed the cosmic-ray distribution needed to account for the gamma-ray results and found that it must be 1.9 to 4.8 times the local solar system value in a region about 5 kpc from the Galactic center.

Later, better information on the atomic and molecular hydrogen densities in the Galaxy became available and a large number of studies of the gamma-ray and matter distributions were made. Most recent studies (e.g., Fichtel & Kniffen 1984; Bloemen, Blitz, & Hermsen 1984; Bhat et al. 1985; Harding & Stecker 1985; Bloemen et al. 1986; Strong et al. 1987, 1988), but not all (e.g., Lebrun et al. 1983) concluded that there was a correlation between the cosmic rays and matter on some scale, as noted above. Among the more recent work, Fichtel & Kniffen (1984), using the spiral arm model of Georgelin & Georgelin (1976) and available matter density information, assumed the cosmic rays to be correlated with matter on the scale of arm segments and obtained reasonable agreement. Harding & Stecker (1985) tried an unfolding method and obtained a correlation between Galactic structural features and cosmic rays showing a strong correlation in the 5 kpc region as well as spiral features. Strong et al. (1988), using a radially symmetric model wherein the Galactic plane is divided into rings, show that, on the average, there is a correlation with a generally decreasing gamma-ray emissivity, and hence presumably cosmic-ray density, with Galactic radius. They also conclude that there is possibly a change in energy spectrum of the gamma radiation with Galactic radius. Because large concentric rings (a few kpc wide) were used, any spiral arm effect is necessarily somewhat suppressed in that model. At the present time, the data are not sufficiently detailed to allow a distinction between coupling on the scale of arms (e.g., Bignami & Fichtel 1974; Fichtel & Kniffen 1984), a general gradient (e.g., Strong et al. 1987, 1988), or some other scale. For a recent review, see Bloemen (1989).

In the present work, the interaction processes producing gamma rays will be discussed first, followed by a summary description of the atomic and molecular hydrogen data to be used. These sections will be followed by a discussion of theoretical considerations related to the interrelationship between Galactic magnetic fields, cosmic rays, and matter. The approach used to incorporate these concepts and the calculations to estimate the gamma-ray production will then be described and developed.

The analysis uses a three-dimensional model of matter, cosmic-ray, and photon densities, and it allows various distribution models of the components to be studied. In particular, a specific case is developed in which it is assumed that cosmic rays are coupled to interstellar matter over a length scale of a few kpc in the plane of the Galaxy. The basis for this assumption stems from consideration of the dynamic balance that exists between the Galactic expansive pressures of cosmic rays, magnetic fields, and kinetic motion of matter, and the attractive gravitational fields. In this analysis, there are only two adjustable parameters; one is the coupling constant between cosmic rays and matter and the other is the parameter to convert CO measurements to molecular hydrogen column densities. Other physical parameters that are used in the calculation are assumed to be adequately well known and not considered adjustable. A set of predictions is then presented and compared to existing data. In addition, the question of the sensitivity of the calculations to changes in various parameters is also studied.

2. INTERACTION PROCESSES PRODUCING DIFFUSE GAMMA RAYS

The basic components for the production of diffuse gamma rays were noted in the introduction to include interstellar matter, cosmic rays, and low-energy photons. Among the interactions that can occur, the three that are dominant include nuclear interactions between cosmic rays and matter, bremsstrahlung collisions between electrons and matter, and inverse Compton scattering of electrons with low-energy photons. Synchrotron emission from electrons in the magnetic field can also give rise to secondary gamma rays, but this effect is estimated to be insignificant. In addition, line emission from dust and grains that are excited by cosmic-ray collisions may contribute to the observed gamma-ray spectrum at discrete energies below a few MeV, below the range of this analysis. Finally, the observed diffuse gamma-ray emission may also have unresolved point sources which could add to the other production mechanisms.

This section reviews, in order of expected importance, the three production processes and source functions that are the basis for estimating the gamma-ray contribution. These functions are incorporated in the model that is described in later sections. For a discussion of the other production mechanisms, see, for example, Fichtel & Trombka (1981).

2.1. *Nuclear Interactions With Matter*

In the high-energy regions of the spectrum above 70 MeV, nuclear interactions between cosmic rays and matter are the most significant mechanism for the production of gamma rays. These collisions produce charged and neutral pion secondaries

whose multiplicities are dependent on the collision energy. Neutral pions decay directly, mostly into two gamma rays, and charged pions decay into electrons and positrons which in turn may annihilate near rest to produce the well-known 0.511 MeV line. Several calculations of the gamma-ray production function from the decay of neutral pions have been made (Carvallo & Gould 1971; Stecker 1970, 1979; Dermer 1986). The more recent results for the differential energy gamma-ray production function, per atom of interstellar material resulting from nuclear interactions is shown in Figure 1 (from Stecker 1988). Notice that the spectrum has a maximum at half the rest mass of the neutral pion, 68 MeV. This function has been parameterized for the local region of the Galaxy for incorporation into the model as follows:

$$q_{\rm nm}(E) = 2.63 \times 10^{-26} \exp\left[-2.36(\ln E) - 0.45(\ln E)^2\right] \ {\rm s}^{-1}\ {\rm GeV}^{-1} \qquad 0.01\ {\rm GeV} < E < 1.5\ {\rm GeV}\ ,$$
$$= 3.3 \times 10^{-26} E^{-2.71}\ {\rm s}^{-1}\ {\rm GeV}^{-1} \qquad 1.50\ {\rm GeV} < E < 7.0\ {\rm GeV}\ ,$$
$$= 4.6 \times 10^{-26} E^{-2.86}\ {\rm s}^{-1}\ {\rm GeV}^{-1} \qquad 7.0\ {\rm GeV} < E\ . \tag{1}$$

The energy E is expressed in GeV, and natural logarithms are used in these relations.

2.2. *Electron Bremsstrahlung Interactions With Matter*

Electrons interact with the interstellar matter to produce gamma rays by the bremsstrahlung process. Based on the cross sections of Koch & Motz (1959), a good approximation to the gamma-ray production spectrum, especially in the case of relativistic electrons is given by

$$q_{\rm em}(E_\gamma, \boldsymbol{r}) = \frac{4\pi}{E_\gamma} \sum_i \frac{\mu_i}{X_{0i}} \int I_e(E_e, \boldsymbol{r}) dE_e\ , \tag{2}$$

where μ_i and X_{0i} are the mass density and radiation length of the ith species of the target medium, and $I_e(E, \boldsymbol{r})$ is the electron differential energy spectrum. The spatial dependence of I_e is denoted by $\boldsymbol{r}$. This expression is evaluated assuming that the interstellar medium has a composition that is predominantly hydrogen, with 10% He and 1% heavier nuclei, and assuming that the electron spectrum is a power law in energy:

$$I_e(E_e, \boldsymbol{r}) = K(\boldsymbol{r}) E_e^{-a}\ . \tag{3}$$

The result, expressed per hydrogen atom, is

$$q_{\rm em}(E_\gamma) = 4.7 \times 10^{-25} K(\boldsymbol{r}) \frac{E_\gamma^{-a}}{a-1}\ {\rm s}^{-1}\ {\rm GeV}^{-1}\ . \tag{4}$$

Considerable uncertainty exists in the electron spectrum for energies below about 5 GeV due to the influence of solar modulation. Fichtel et al. (1991) estimated the local electron spectrum. At energies below 70 MeV where bremsstrahlung is the dominant process, they used gamma ray observations, and at intermediate energies, the spectrum shape was inferred from synchrotron data. Their results join with direct observations of the electron primary spectrum at high energies. For the purposes of this analysis, their spectrum is well represented by a power law in energy with a break in index from 2.35 to 3.3 at 5 GeV. This spectrum, together with the bremsstrahlung cross section, results in bremsstrahlung source functions per atom in the local region of the Galaxy:

$$q_{\rm em}(E_\gamma) = 4.4 \times 10^{-27} E_\gamma^{-2.35}\ {\rm s}^{-1}\ {\rm GeV}^{-1} \qquad 0.010\ {\rm GeV} < E_\gamma < 5\ {\rm GeV}\ ,$$
$$= 2.1 \times 10^{-26} E_\gamma^{-3.3}\ {\rm s}^{-1}\ {\rm GeV}^{-1} \qquad 5\ {\rm GeV} < E_\gamma < 40\ {\rm GeV}\ . \tag{5}$$

The bremsstrahlung production function is compared with the nuclear interaction production function in Figure 1.

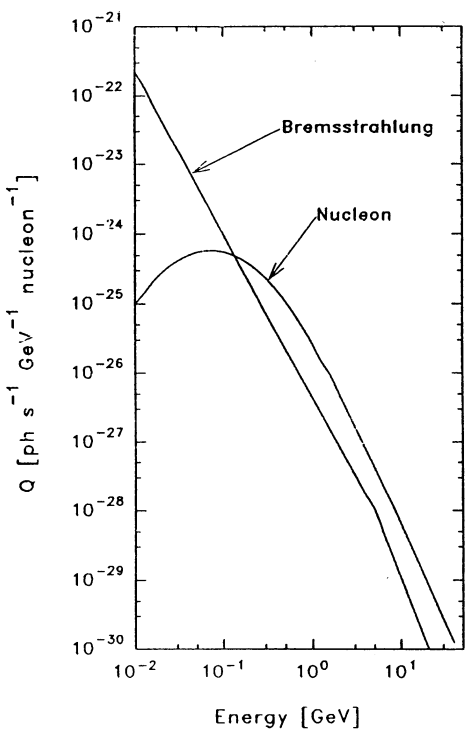

FIG. 1.—Gamma-ray source functions for nucleon-nucleon interaction and electron bremsstrahlung process used to calculate gamma-ray production from cosmic-ray interactions with interstellar matter.

2.3. *Inverse Compton Interactions*

Cosmic-ray electrons interact with the interstellar radiation field and produce gamma rays through the inverse Compton interaction. Mathis, Mezger, & Panagla (1983) developed a stellar model consisting of four components covering the wavelength region from 0.1 to 8 μm to which the far-infrared (8 to 1000 μm) and blackbody populations must also be added. The energy densities of these components will be discussed further in § 3.4.

The source functions, $q_{\rm pi}(E_\gamma, \boldsymbol{r})$, are

$$q_{\rm pi}(E_\gamma, \boldsymbol{r}) = \frac{8\pi}{3} \sigma_{\rm T} \left(\frac{4}{3} \langle \epsilon_i \rangle\right)^{(a-3)/2} (mc^2)^{(1-a)} K(\boldsymbol{r}) E_\gamma^{-(a+1)/2}\ , \tag{6}$$

assuming a power-law spectrum for the electron differential energy of the form given above. (See, for example Ginzburg & Syrovatskii 1964). Here, ϵ_i represents the energy of the interstellar photons, $\sigma_{\rm T}$ is the Thompson cross section and $q_{\rm pi}$ when

multiplied by the radiation field energy density has units of (area time energy solid angle)$^{-1}$.

Gamma rays produced from the inverse Compton process have an energy that scales from the electron and photon energy according to

$$\langle E_\gamma \rangle = \frac{4}{3}\left(\frac{E_e}{mc^2}\right)\langle \epsilon_i \rangle \quad (7)$$

where E_γ, E_e, and ϵ_i are the gamma-ray, electron, and photon energies, and mc^2 is the electron rest energy. Consequently, very high-energy electrons are required to produce gamma rays. For example, a 100 MeV gamma ray produced by this mechanism requires an electron of energy from 1 to 300 GeV, depending on the target photon energy. The electron spectrum of Fichtel et al. (1991), used above in developing the bremsstrahlung source function has a slowly changing index in the vicinity of 5 GeV. However, equation (6) can still be used to a good approximation by choosing the index appropriate to the photon energies of interest.

3. DISTRIBUTION OF GALACTIC MATTER AND PHOTONS

The dominant constituents of the interstellar medium (ISM) are hydrogen gas, primarily in atomic and molecular form, and the interstellar dust with which it is mixed. In terms of both total mass and target particles for cosmic ray interactions, it is the hydrogen gas which is of prime importance in the production of diffuse gamma-ray emission in the Galaxy. In this section we briefly review the Galactic distribution of matter as revealed by radio surveys of the Galaxy in the spectral lines of atomic hydrogen (H I) and carbon monoxide (CO). A model of the H II component is included, based on recent work by Taylor & Cordes (1993). Owing to its small contribution to the production of diffuse gamma-ray emission, a discussion of the dust component of the ISM is neglected. Further, the analysis is restricted to the matter distribution within 10° of the plane of the Galaxy, deferring a discussion of the possible extension of the present work to high Galactic latitudes to a later paper.

The distribution of interstellar matter in Galactic azimuth and radius is deduced from the observed radial velocity of the emitting gas after application of a model of circular Galactic rotation. Beyond the solar circle in the outer Galaxy, where the gas is mainly atomic, there is a one-to-one correspondence between Galactic radius and line-of-sight distance. However, in the inner Galaxy, where molecular gas is an important constituent, two distances correspond to a given Galactic radius. For this latter case, assumptions must be made regarding the near-far distribution or, where possible, secondary distance indicators must be used (e.g., associated Population I objects, Galactic latitude or angular size, optical or near-infrared extinction) to resolve the ambiguity. Departures from strict circular symmetry (e.g., gas streaming motions) introduce systematic errors in the Galactic matter distribution deduced from radio observations, and absolute mass determinations from integrated spectral line profiles also may be affected by optical depth and temperature effects. For a detailed discussion of these topics see Mihalas & Binney (1981), Kulkarni & Heiles (1988), and Burton (1988).

The contribution of other constituents of the interstellar medium is small. Whereas ionized matter, grains, and dust are negligible from the standpoint of high-energy gamma-ray production, except for the possibility of gamma-ray lines from interstellar grains, helium and heavier nuclei do contribute significant additions to the diffuse gamma-ray intensity. They represent about 10% and 1% of the hydrogen content, respectively. Since little is known about their distribution, the local values are used and are included as multiplying factors in the production functions, as noted in § 2.

3.1. *Atomic Component*

The distribution of atomic hydrogen (H I) in the Galaxy has been well mapped at radio wavelengths in the 21 cm hyperfine transition (for recent reviews see Burton 1988; Dickey & Lockman 1990). In general, the atomic gas is much more extended throughout the disk of the Galaxy than either molecular or ionized hydrogen. The radial scale length of H I is also greater by about a factor of 2 than that of typical components of Population I objects. In the inner Galaxy, H I structures are generally confined to a thin flat layer whose average half-thickness at half-density points is about 106 pc at $R < 8.5$ kpc (Lockman 1984). Perpendicular to the Galactic plane, the density distribution is approximately Gaussian with low-intensity wings extending to higher distances perpendicular to the plane. The H I layer in the outer Galaxy deviates markedly from a flat disk. The observed warp of H I gas from the equatorial plane of the Galaxy is toward positive Galactic latitudes in the northern sky (the first and second quadrants of the Galaxy) and toward negative latitudes in the south (third and fourth quadrants). The H I layer remains flat until about 12 to 13 kpc from the Galactic center where the amplitude of the warp grows approximately linearly until about $R = 16$ kpc. At larger radii, the warp of the H I in the northern hemisphere continues to rise, while in the south, the gas attains its largest displacement from the plane at a distance of approximately $R = 18$ kpc. In both hemispheres, however, the gas layer is observed to flare at large Galactocentric radii; the scale height in the warped layer at $R = 25$ kpc is approximately an order of magnitude greater than it is near the solar circle (Burton 1988; Wouterloot et al. 1990).

The total mass of the Galaxy in H I is estimated to be $\sim 5 \times 10^9\ M_\odot$, of which 80% or more resides in the outer Galaxy (Henderson, Jackson, & Kerr 1982; and Wouterloot et al. 1990). Table 1 summarizes the main characteristics of the atomic hydrogen component of the interstellar medium.

3.2. *Molecular Component*

The distribution of molecular hydrogen is usually inferred from the tracer molecule carbon monoxide (CO) and requires estimation of a conversion factor relating the observed integrated CO intensity to molecular hydrogen column density. Factors which may affect the interpretation of CO observations include elemental and isotopic abundance ratios, as well as temperature and optical depth effects. (See, e.g., Kutner & Leung 1985; Maloney & Black 1988.) On a Galactic scale, the abundance ratio of CO to H_2 apparently remains fairly constant over a wide range of interstellar conditions, and the $J = 1 \rightarrow 0$ rotational transition of CO at 115 GHz, readily detected at millimeter wavelengths at 2.6 mm, has become the molecular analog of the 21 cm atomic hydrogen line for large-scale studies of interstellar gas in the Galaxy. The present discussion of the distribution of molecular material in the ISM is based on the results of the Columbia CO survey with an antenna of 1.2 m aperture at Columbia University in New York City, now at the Center for Astrophysics in Cambridge, and a twin instrument located on Cerro Tololo in Chile. The culmination of this low-resolution CO work is a composite

TABLE 1

CHARACTERISTIC PROPERTIES OF ATOMIC AND MOLECULAR COMPONENTS OF THE INTERSTELLAR MEDIUM

Parameter	Atomic	Molecular
Typical Structures	Filaments, loops, shells	Clumps, GMC's
Temperature (K)	20–$\approx 10^2$	3–30
Mean Density (cm^{-3})	$n(H\ I) \approx 0.1$ to 1 cm^{-3}	$n(H_2) \approx 10^2$–10^5 cm^{-3}
Local Density (atom cm^{-3})	≈ 0.45	≈ 0.2
Layer Radial Extent (kpc)	3–25	3–8
($R_\odot = 8.5$ kpc)	(warped for $R > 11$ kpc)	
Total Mass ($M_\odot$)	$\approx 5 \times 10^9$ ($\approx 80\%$ at $R > R_\odot$)	≈ 0.8–1.4×10^9 ($\approx 14\%$–50% at $R > R_\odot$)

map at 0°.5 resolution of the molecular clouds in a thick band along the Milky Way, described in detail in Dame et al. (1987).

Approximately half the hydrogen gas within the solar circle is in molecular form. The H_2 gas is more highly concentrated toward the inner Galaxy than the atomic hydrogen and most dense in a "molecular ring" between 4 and 8 kpc in Galactocentric radius. Its half-thickness with respect to distance above and below the plane, approximately 60 pc, in contrast to that of H I, is close to that of the Population I stars, underscoring the intimate relationship between molecular clouds and regions of star formation. From a joint analysis of the northern and southern CO surveys, Bronfman et al. (1988) derived a total molecular mass for the region between $R = 2$ kpc and the solar circle. Their value, after scaling for $X = 2.3 \times 10^{20}$ molecules cm^{-2} (K km $s^{-1})^{-1}$ and $R_0 = 8.5$ kpc, is $7 \times 10^8\ M_\odot$. Recent estimates place the total amount of molecular material at $R > 11$ kpc in the range (1–7) $\times 10^8\ M_\odot$ (Digel, Bally, & Thaddeus 1990; Wouterloot et al. 1990).

From a comparison of the Columbia CO survey, 21 cm atomic hydrogen surveys, and the Galactic diffuse high-energy gamma ray emission observed by *COS B*, the important conversion ratio X between the H_2 column density and the observed velocity-integrated CO line emission, required to derive the mass of molecular clouds, has been calibrated over much of the Galaxy. The result of this analysis by Strong et al. (1988) is $X = N(H_2)/W_{CO} = 2.3 \pm 0.3 \times 10^{20}$ molecules cm^{-2} (K km $s^{-1})^{-1}$, in agreement with the range of values (1–4) $\times 10^{20}$ using other methods, such as star counts and the virial theorem (Solomon & Barrett 1991). However, as Strong et al. (1988) noted, if unresolved point sources having a similar distribution to that of H_2 exist, then the actual value of X would be less. In addition, it should be emphasized that a Galactic average value is being used, and that for specific molecular clouds, the value might be quite different.

High-resolution radio observations of external spiral galaxies indicate that the arm–interarm contrast of the molecular gas traced by CO is generally higher than that of the atomic gas (Casoli 1991). Estimating arm–interarm contrasts in our own Galaxy is more difficult, but at Galactic radii where molecular clouds are neither too sparse to trace the arms well ($R < 12$ kpc) nor so numerous as to be severely blended ($R > 6$ kpc), a number of well-defined "grand design" spiral features have been identified (Dame et al. 1986; Grabelsky et al. 1988). The Perseus and Carina arms in the outer Galaxy, for example, are particularly well defined in molecular clouds, and, in the Local neighborhood, nearly all the clouds within 1 kpc in the first and fourth quadrants apparently lie on a fairly straight ridge more than 1 kpc long which may trace the inner edge of a Local spiral arm or spur (Dame et al. 1987).

Although results for the inner Galaxy are much less satisfactory, owing to the well-known problem of the twofold kinematic distance ambiguity for clouds within the solar circle, it has been shown that the Sagittarius arm in the first Galactic quadrant is fairly well defined by large clouds (Dame et al. 1986; Clemens et al. 1988; Solomon & Rivolo 1989) and that it may join the Carina Arm in the fourth quadrant to constitute a single feature at a pitch angle of about 10° extending nearly three-quarters of the way around the Galaxy (Grabelsky et al. 1988). To date, this well-known problem of distance ambiguity has been resolved with a high degree of confidence for only the largest and most prominent molecular complexes in the inner Galaxy (e.g., Dame et al. 1986), because they are the most well defined and are associated with a variety of Population I objects. More than half the total molecular mass is contained in smaller clouds, or in very complicated regions where identification of individual objects is difficult. Table 1 summarizes the main characteristic properties of the molecular component of the ISM.

3.3. *Surveys Used in the Present Work*

The atomic hydrogen (H I) data used in the present analysis were taken from the following sources. In the Galactic plane ($|b| \leq 10°$) the northern H I survey of Weaver & Williams (1973) ($l = 10°$ to 250°) has been combined with the Maryland-Parkes southern H I survey (Kerr et al. 1986; $l = 240°$ to 350°) to obtain a uniform H I map at a grid spacing of 0°.5 in longitude and 0°.25 in latitude. The region of the Galactic center ($l = 350°$ to 10°) was extracted from the Leiden-Green Bank Galactic H I survey (Burton & Liszt 1983; Burton 1985) at slightly reduced spatial resolution (1° spacing in l and b). Stark et al. (1992) recently conducted a survey of H I for latitudes above $-40°$. These measurements are relatively free of sidelobe contamination that can be significant in regions of sky with low column density, specifically regions well removed from the plane. The Stark et al. (1992) results were not used, however, since their resolution is only 2 degrees and, according to these authors, filter bank saturation can cause inaccuracies in regions within 5 degrees of the plane—the region of most interest here.

A model of ionized hydrogen is incorporated using the fitted distribution developed by Taylor & Cordes (1993) based on studies that correlate observed pulsar dispersion for pulsars of known distance, and on interstellar scattering measures of both Galactic and extragalactic sources. Their model accommodates spiral arm features determined from radio and optical observations, and does not assume axisymmetry in the Galaxy. As will be seen later, the contribution to the diffuse gamma-ray intensity from H II is small compared to that of H I and H_2.

The CO observations employed to deduce the distribution of molecular hydrogen within the plane of the Galaxy are those described in Dame et al. (1987). This composite CO survey covers the entire Galactic plane at a resolution of 0°.5. The coverage in Galactic latitude for this survey is typically 10°, extending in certain regions (e.g., the Orion and Ophiucus star-forming regions) to 25°.

3.4. *Interstellar Radiation Field*

The interstellar photon densities that are of interest in calculating the inverse Compton contribution are primarily the cosmic microwave background and the infrared, optical and ultraviolet radiation that arise from within our Galaxy. To perform the calculation, it is necessary to model the spatial distribution and spectrum of each of these photon populations. The cosmic blackbody radiation is taken to be 2.7 K everywhere with a photon energy density of 0.25 eV cm^{-3}. The far-infrared (FIR) photon radial distribution is taken from the cold dust emission curve of Cox, Krügel, & Mezger (1986); the decrease with height above the plane of the Galaxy is approximated by an exponential distribution characterized by a scale height of ~ 0.1 kpc. The distribution is then normalized so that the total integrated FIR luminosity of the Galaxy is 1.5×10^{10} $L_\odot$ (Cox et al. 1986). The interstellar radiation field in the near infrared, optical, and ultraviolet adopted here are taken from the work of Chi & Wolfendale (1991), who used the stellar model of Mathis, Mezger, & Panagla (1983) with four stellar components emitting in the range of $8 < \lambda < 1000$ μm. The distribution corresponding to a solar radius of 8.5 kpc (Kerr & Lynden-Bell 1986) is adopted for use here.

4. INTERRELATIONSHIP BETWEEN COSMIC RAYS AND MATTER

The distribution of cosmic rays, in contrast to those of matter and photons, has not been and probably will not be directly measured due to their interaction with magnetic fields. This section gives theoretical arguments that guide the construction of a cosmic-ray spatial distribution model. The first question to be addressed is whether the cosmic rays are Galactic or universal, or possibly constrained to some large volume. At this time, there is no compelling evidence that the cosmic rays are not universal, but there are several arguments against this idea. One is that the Compton interactions with the blackbody radiation would seriously degrade the electron spectrum over the lifetime of the Galaxy. Further, there seems to be great difficulty in finding any acceptable source for the cosmic rays in this case unless they are primordial. The age of the cosmic rays based on isotopic composition studies is estimated to be slightly more than 10^7 years and the secondary abundances are consistent with that age, the matter density in the Galaxy, and a Galactic origin. The present gamma-ray data suggests that the cosmic rays are not uniform in their spatial distribution (e.g., Fichtel 1989). In addition, the cosmic ray density is close to the maximum that can be contained by the uniform Galactic magnetic field. Hence, it seems reasonable to assume that the cosmic rays are Galactic in nature, and if so it is likely that they play an important role in the considerations of Galactic dynamic balance. The validity of this assumption will, of course, be tested by the model being described here. Implications of alternate assumptions, including an extragalactic origin for the cosmic rays will also be considered.

Assume for the moment that the cosmic rays are Galactic and consider the question of the dynamical balance between the interactions of cosmic rays, magnetic fields, and gravitation attraction of the matter in the Galaxy. Under the assumption that (1) the external pressures are small compared to the Galactic magnetic field and cosmic ray pressures in the disk (i.e., that the cosmic rays are Galactic and not universal), (2) the cosmic rays and magnetic fields are in a quasi-stationary state for which there is good experimental evidence (Parker 1969), and (3) the Galactic magnetic field is confined to the disk by the interstellar gas rather than being force-free with the confinement being in a distant place such as the Galactic center, Parker (1966, 1969, 1977) following earlier work by Bierman & Davis (1960) showed that the magnetic fields and cosmic rays must be confined to the Galaxy by the weight of the gas threaded by the field.

In addition, the cosmic-ray pressure may not exceed the magnetic field pressure (Parker 1968). As long as the cosmic-ray source strength is sufficiently large, the cosmic ray pressure will be about as large as the magnetic fields can hold. The magnetic field then acts as a safety valve. Because of irregularities and fluctuations, it might be suspected that the cosmic-ray pressure normally does not quite reach that of the magnetic field on the average. A recent analysis of estimates of the cosmic-ray and magnetic field pressures locally in our Galaxy by Fichtel et al. (1991) suggest that this, in fact, is the case. Further, observational evidence suggests that there is approximately enough gas locally in the Galaxy to provide a balance for the three pressures. A large body of data suggests that the cosmic ray density locally has varied little over the last 10^4 to 10^9 years (Parker 1969). Hence, the balance and quasi-equilibrium assumptions seem valid.

If the solar system is not in an unusual position in the Galaxy, these features suggest that the cosmic-ray density throughout the Galaxy may be generally about as large as could be contained under near-equilibrium conditions. Further theoretical support is given to the concept by the calculated slow diffusion rate of cosmic rays in the magnetic fields of the Galaxy and the small cosmic-ray anisotropy. These considerations then lead to the hypothesis that the energy density of the cosmic rays is larger where the matter density is larger on some coarse scale.

The picture that emerges then is that cosmic rays, at least below 10^{16} or 10^{17} eV per nucleon, are bound to the lines of force, and the field lines are normally closed (or else the cosmic rays would escape too quickly). The cosmic rays are constrained and not free to escape individually. Thus, if they do escape, it must be the result of cosmic-ray group pressure inflating the magnetic field lines and pushing outward from the Galaxy. All cosmic-ray particles then, whether they have 1 GeV, 10^2 GeV, or 10^4 GeV, escape with about equal ease. (See e.g., Parker 1966, 1969, 1977.) The modest variation in path length of the cosmic rays with energy supports this concept, and the path length variation which is seen could be largely the result of source location and local diffusion, rather than escape.

Within the context of the above discussion, an unanswered question is the scale of the coupling between cosmic rays and matter. Synchrotron measurements suggest a scale height for the magnetic fields and cosmic rays perpendicular to the plane of about 1 kpc. Calculations of the diffusion rate of cosmic rays in the Galaxy also suggest that the scale may be of this order, or somewhat larger. Galactic arm widths and large clouds may also suggest a coupling scale in the range of a half to a few kpc in the plane. Disturbances, such as supernovae, suggest the scale is probably not smaller than about a half kpc. A purely

theoretical approach to obtain an answer to the question of the scale size seems not to be possible because too much is unknown, although arguments exist against the scale size in our Galaxy being the largest possible, i.e., the Galaxy as a whole (See Parker 1966). An experimental measurement may be the best approach to an answer to this question. Hence, in this work, it is left as an adjustable parameter.

5. PRESENT MODEL

A goal of this investigation is to provide the mechanism for making a more detailed prediction of the cosmic-ray distribution in the Galaxy which may be compared to experimental results, thereby testing the basic theories of dynamic balance and cosmic-ray containment. To this end, the model presented here for the calculation of the high-energy diffuse gamma-ray emission from the Galaxy is based on the full Galactic matter distribution described in § 3. It allows for the separation of the near and far components along a given radial line of sight. The cosmic-ray distribution, as will be seen in the following subsection, may vary both with radial distance from the Galactic center and Galactic azimuth. Hence, not only are nonsymmetric distributions relative to the Sun permitted, but also variations in azimuth for a given Galactic radius and in fact any deduced distribution within the limits allowed by observed data.

The intensity of diffuse Galactic gamma rays of energy E_γ from Galactic longitude l and latitude b is expressed in a general form by

$$j(E_\gamma, l, b) = \frac{1}{4\pi}\int [c_e(\rho, l, b)q_{\rm em}(E_\gamma) + c_n(\rho, l, b)q_{\rm nm}(E_\gamma)] \times [n_{\rm H\,I}(\rho, l, b) + n_{\rm H\,II}(\rho, l, b) + n_{\rm H_2}(\rho, l, b)]d\rho + \frac{1}{4\pi}\sum_i \int c_e(\rho, l, b)q_{\rm pi}(E_\gamma, \rho)u_{\rm pi}(\rho, l, b)d\rho \quad \gamma\ {\rm cm}^{-2}\ {\rm s}^{-1}\ {\rm sr}^{-1}\ {\rm GeV}^{-1}\ . \quad (8)$$

The integrations are over line-of-sight distances along l and b from the solar region, denoted by ρ. The first integral represents the production of cosmic-ray interactions with matter where $q_{\rm em}$ and $q_{\rm nm}$ are the production functions per target atom based on the local cosmic-ray density and given by equations (1) and (5) for electron and baryon interactions. The functions $c_e(\rho, l, b)$ and $c_n(\rho, l, b)$, discussed in § 3.1 below, are ratios of the electron and nucleon cosmic-ray intensities relative to the local intensities. These functions could also depend on energy if the spectral indices vary with location in the Galaxy. Observations at 408 and 1420 MHz by Reich & Reich (1988) show that spectral variations occur particularly when high latitudes are compared with values in the plane. In the region of the plane appropriate for this work, the indices range from 2.85 to 3.1. Bloemen et al. (1988) infer that cosmic-ray nucleons have spectral indices that vary at high latitudes, but are relatively constant near the plane. Spectral variations, as well as differences in the electron-to-proton ratio are thought to be negligible based on a study of lifetime and secondary production (Fichtel & Kniffen 1984). These considerations allow the cosmic-ray density at any location (ρ, l, b) to be written as a multiplying scale factor relative to Local solar neighborhood values in equation (8), and in addition,

$$c_e(\rho, l, b) = c_n(\rho, l, b) \equiv c(\rho, l, b)\ .$$

The quantities $n_{\rm H\,I}(\rho, l, b)$ and $n_{\rm H_2}(\rho, l, b)$ are the atomic and molecular hydrogen densities expressed as atoms per unit volume.

The second term in equation (8) describes the contribution from inverse Compton interactions between electrons and photons. The summation is over the discrete wavelength bands discussed in § 3.4. The production function $q_{\rm pi}(E_\gamma, r)$ is given in equation (6) for the local electron intensity. The photon energy density distributions $u_{\rm pi}(r, l, b)$ (i denotes the wavelength band.) were discussed in § 3.4.

By way of nomenclature, r is the distance from the solar system to an arbitrary point in the plane, z is a measure above and below the plane, R is measured from the Galactic center to a point in the plane, and R_0 is distance measured in the plane from the Sun to the Galactic center. These quantities are related by

$$R^2 = r^2 + R_0^2 - 2rR_0\cos(l); \quad z = \rho\sin(b); \quad \text{and} \quad r = \rho\cos(b) \quad (9)$$

In order to evaluate the integral in equation (8), the Galaxy was divided into cells using a spherical coordinate system centered on the Sun. Cells of size $\Delta l = 0.^\circ5$, $\Delta b = 0.^\circ5$ and, $\Delta\rho = 0.5$ kpc were used based on the angular grid of the radio data. Since each cell is considered separately, no symmetry is assumed with respect to the Galactic center as occurs when a fully concentric ring model is used. This is important in view of the known concentrations of matter in spiral arms.

The details of how the matter density observations are incorporated into the calculation, and how the model used to describe the cosmic-ray distribution are given in the next two subsections.

5.1. *Matter Distribution*

The distribution of atomic and molecular gas is determined from data taken by the various surveys discussed in §§ 3.1 and 3.2. The matter as a function of distance from the Sun in any direction is estimated by dividing the distance into intervals corresponding to a velocity interval. A Galactic rotation curve of Burton & Gordon (1978), modified to a solar radius of 8.5 kpc and parameterized by Clemens (1985) is used to determine the line-of-sight distances corresponding to each of these velocity intervals. Kulkarni, Blitz, & Heiles (1982), and more recently Fich, Blitz, & Stark (1989) suggested corrections to this rotation curve which are significant in the outer Galaxy ($R > 10$ kpc). In the local frame of reference, the relative component of velocity along a line of sight corresponding to a given Galactocentric radius is

$$v(l, R) = R_0\sin(l)[\Omega(R) - \Omega(R_0)]\ , \quad (10)$$

where $\Omega(R_0) = +25.88$ km s^{-1} kpc^{-1} and $R_0 = 8.5$ kpc. The maximum radius used in this analysis is 20 kpc.

The observed integrated intensity of 21 cm line emission over a velocity range (with the corresponding distance interval given by eqs. [9] and [10]) is related to the line-of-sight density of hydrogen atoms for that interval by

$$N_{\rm H\,I}[v(i+1), v(i)] = (1.83\times 10^{18})\int_{v(i)}^{v(i+1)} T_s\,\tau(v)dv\ , \quad (11a)$$

where

$$\tau(v) = -\ln[1 - T_b(v)/T_s] \quad \text{and} \quad T_s = 125\ K\ .$$

Here T_b is the observed brightness temperature, $\tau(v)$ is the optical depth, and T_s is the mean spin temperature. The units are atoms cm^{-2} when velocity is measured in km s^{-1} and temperature in degrees Kelvin. Similarly, the molecular hydrogen line-of-sight density is

$$N_{H_2}[v(i+1), v(i)] = X \int_{v(i)}^{v(i+1)} T_b(v)dv \qquad (11b)$$

The parameter X that relates the integral CO line intensity to the density of molecular hydrogen was discussed at length in § 3.2. It was argued that it ranges from (1–4) × 10^{20} with a nominal value of 2.3 × 10^{20} in units of molecules cm^{-2} (K km s^{-1})$^{-1}$. This quantity is left at this point as a free parameter within the constraints just mentioned.

For values of $R > R_0$ in equation (10), the relationship between R and v is unique. For these cases, the quantities $N_{H\,I}$ and N_{H_2}, apart from a factor of $\Delta\rho$, are the matter density functions required in equation (8). In the inner Galaxy, however, a line-of-sight intersects a circle of radius R at two locations so that there are two solutions for ρ for a given velocity, and the quantities $N_{H\,I}$ and N_{H_2} are the totals for the two regions. For these cases, it is necessary to distribute the matter between the near and far locations. Detailed information on how matter is divided between the two regions in the inner Galaxy is not available. For the purposes of numeric evaluation, a weighting scheme was adopted based on an assumed Gaussian distribution of matter normal to the plane. For a given line of sight, the heights above the plane at the center of the two cells corresponding to the distance-region solutions of equation (10) are used to calculate Gaussian amplitudes, and these are used to establish weighting functions:

$$\eta(\rho_1) = \frac{\exp\left[-0.5\rho_1^2 \sin^2(b_1)/Z^2\right]}{\exp\left[-0.5\rho_1^2 \sin^2(b_1)/Z^2\right] + \exp\left[-0.5\rho_2^2 \sin^2(b_1)/Z^2\right]}$$

$$\eta(\rho_2) = 1 - \eta(\rho_1)\,. \qquad (12)$$

In the special case of $b = 0$, the weight factors reduce to 0.5 so that matter is distributed equally between the near and far points. The width of the Gaussian Z is taken to be 106 pc for atomic hydrogen and 60 pc for molecular hydrogen as was discussed in § 3.1 and § 3.2. Since the weighting is only needed in the inner Galaxy, it is not affected by the increasing disk thickness that occurs outside the solar circle.

The mass density functions in equation (8) are then

$$n_{H\,I}(\rho_1, l, b) = \frac{\eta(\rho_1) \times N_{H\,I}}{\Delta\rho_1} \qquad (13)$$

and likewise for the second region, ρ_2, and similarly for n_{H_2}, whereas in the outer Galaxy, $\eta = 1$.

The kinematic deconvolution of the radio data is not possible for line-of-sight directions near the Galactic center or anticenter. For the zones $|l| < 10°$ and $|l - 180°| < 10°$, the observed column densities are given the same relative distance distribution as the average of six bins (3°.0) on either side of the zones at the same corresponding latitude. Within 10° of the Galactic center, the CO observations show gas with very high velocity (see Dame et al. 1987, Fig. 3) that requires special treatment. The optical depth of this gas is likely to be significantly less than average (particularly if the high velocities indicate turbulence in the molecular gas). If this is true, the Galactic average conversion factor from $W(CO)$ to $N(H_2)$ that applies for optically thick conditions will greatly overestimate the molecular hydrogen column density. To avoid this overestimation when correcting the interpolated column density, upper v_{max} and lower v_{min} velocity limits

$$v_{max} = 2.4(l + 60) + 12.4 \text{ km s}^{-1}; \quad -6° < l < 10°$$

$$v_{min} = -39.2 \text{ km s}^{-1}; \quad -2° < l < 2°$$

were used in the longitude ranges specified. For all other longitudes, the full velocity range of the radio data were used.

5.2. *Cosmic-Ray Distribution*

In this section, a specific assumption will be made for the cosmic-ray density distribution based on the discussion of § 4, namely that on a coarse scale the energy density of cosmic rays is larger where the matter density is larger. This correlation can be discussed in terms of a region size that describes the matter that influences the cosmic-ray density at a given location. The correlation could be extremely tight in which case a simple proportionality would exist between matter and cosmic-ray densities. At another extreme, the matter in the whole Galaxy affects cosmic rays so that their density would be a relatively smooth symmetric function. These situations would be described as coupling scales of zero on the one hand, and the radius of the Galaxy itself on the other hand. Indeed, cosmic rays could be uniformly distributed in which case an infinite length would apply. In the discussion of this section, cosmic rays are assumed to be related to the matter density smoothed over a region whose size is left as an adjustable parameter. In § 6 where results are discussed, it will be seen that the region size of 2–3 kpc appears to best-fit existing observations. The case of a uniform cosmic-ray intensity is also shown there.

The cosmic-ray density distribution is derived by convolving the surface density of matter (integrating the volume density over the thickness of the Galactic disk) with a Gaussian distribution whose width is an adjustable parameter r_0 referred to as the scaling length. This approach is taken since it is the total Galactic plane mass that is relevant for cosmic-ray containment, and in addition, the scale height of cosmic rays is large compared to matter so that the variation of cosmic-ray density with height is not important. The convolved distribution is normalized to the local matter density. Hence,

$$c(\rho, l, b) = \frac{\mu_{cr}(r, l, b)}{\mu_{cr,\,local}} = \left[2\pi r_0^2 \int \mu_m\, dz\right]_{local}^{-1} \iiint \mu_m(r', l', z)dz \times \exp\left(-\zeta^2/2r_0^2\right)\zeta\, d\zeta\, d\psi\,, \qquad (14)$$

where μ_{cr} and μ_m are the cosmic-ray and matter densities, respectively, the subscript *local* refers to the solar neighborhood value, and radius ζ and angle ψ relate the points (r, l) and (r', l') by

$$r'^2 = r^2 + \xi^2 - r\zeta\cos(\psi) \quad \text{and} \quad \cos(l' - l) = \frac{r'^2 + r^2 - \zeta^2}{2rr'}\,.$$

The radio observations generally cover the range $|b| < 10°$, and for regions that are nearby, the full thickness of the plane is not sampled. When this occurs, the evaluation of the integrals $\int \mu_m\, dz$ require special treatment. Here, the density of matter in the unsampled region is extended from the sampled region using Gaussian distributions characterized by the scale heights of each gas component. In the inner Galaxy, the scale height of

the matter is taken to be constant at 110 pc for atomic and 60 pc for molecular hydrogen. For the outer Galaxy, the scale height of atomic hydrogen slowly increases as a function of the Galactocentric radius R. Molecular hydrogen is a relatively small constituent, typically about 1/6th by mass, and the scale height varies relatively little. In the outer Galaxy, the scale height of the atomic mass distribution adapted from Burton (1988) by adjusting the solar radius from 10 to 8.5 kpc is represented parametrically by

$$Z_{\rm H\,I} = 55.1955 - 22.4710R + 3.61766R^2 - 0.288585R^3 + 0.011439R^4 - 0.0001791R^5 \text{ kpc}, \quad (15)$$

where R is in kpc. For large values of $R > 17$ kpc, a constant value of $Z_{\rm H\,I} = 2.0$ kpc is used.

Shull & Van Steenberg (1985), using the *International Ultraviolet Explorer* satellite, studied the neutral hydrogen abundance in the local interstellar medium and obtained a mean number density of 0.46 H I atom cm^{-3}. From a study of molecular hydrogen gas within 1 kpc of the Sun, Dame et al. (1987) obtained a mean molecular hydrogen density of 0.2 atom cm^{-3}. For this model, the value adopted for total gas in the local region is the sum of these two results, or 0.66 atom cm^{-3}. As a check, the procedure outlined above was applied to the local region within 1 kpc of the Sun. The volume densities of H I and H_2 were found to be in reasonably good agreement ($\approx$40%) of adopted values. The corresponding surface density is 1.2×10^{20} atoms cm^{-2}. (The correction for heavier elements is included in q as described in § 2.)

5.3. *Approach to Parameter Determination*

In this work, there are two parameters that are considered to be adjustable. On the basis of what is known at present, each one is only adjustable within certain allowed limits. The two are X, the normalization factor used to convert the CO measurements to molecular hydrogen column density and, r_0, the scale of coupling of the cosmic rays to matter. The scale r_0 will be allowed to vary in the range from $\frac{1}{2}$ to 6 kpc. Values much less than about $\frac{1}{2}$ kpc seem improbable because of the scale height of cosmic rays perpendicular to the plane is estimated to be that value from synchrotron data, and the scale in the plane would not be expected to be smaller. Further, the results to be studied are insensitive to scales much smaller than $\frac{1}{2}$ kpc. At the other end, coupling much larger than about 6 kpc would in effect consider the Galaxy as a whole. However, it should be remembered that for the reasons given by Parker (1966) and very briefly summarized earlier in this paper, the scale of the Galaxy as a whole is not believed to be a correct alternative. The constant cosmic-ray case is treated as a special case. Following the discussion in § 3.2, the value of X is considered to be an adjustable parameter in the range $(1\text{–}4) \times 10^{20}$ molecules cm^{-2} (K km s^{-1})$^{-1}$.

By adjusting the parameters of the calculation and making comparisons with past and future high-energy gamma-ray measurements, it should be possible to obtain a measure of the scale of coupling, to obtain a better estimate of the molecular hydrogen normalization, and in the future to determine the special role of clouds if any. The other important aspect of this work is to establish a method of testing for the accuracy and uniqueness of conclusions and the sensitivity to the variation of parameters.

The only complete maps of the Galactic plane in high-energy gamma rays ($E > \sim 50$ MeV) that exists, were obtained by the *SAS 2* and *COS B* satellites. *SAS 2* was launched into a circular, low-altitude equatorial orbit and it had a relatively short lifetime of about $6\frac{1}{2}$ months due to an electronics part failure, while the later experiment *COS B* was placed into a highly eccentric orbit and provided data for over 6 years. *SAS 2* had an extremely low instrumental background (Fichtel et al. 1978). A small contribution to the measured Galactic plane emission is expected from the isotropic extragalactic diffuse emission, which is determined from the *SAS 2* results (Fichtel et al. 1978; Thompson & Fichtel 1982) to be $\sim 1.2 \times 10^{-5}\ \gamma(E > 100$ MeV) cm^{-2} s^{-1} sr^{-1}. Due to the difference in instrumental design and the orbit of *COS B*, the instrumental background was quite high, estimated to be between 1 and 2 times the extragalactic diffuse intensity (and hence more than 60 times the average background of *SAS 2*). The separation of the instrumental and isotropic components measured by *COS B* is therefore not possible, and only the combined instrument plus isotropic background estimates have been published (Mayer-Hasselwander 1985).

In order to compare the model predictions with *SAS 2* and *COS B* results, the contribution from the isotropic component for *SAS 2* ($\sim 1.2 \times 10^{-5}\ \gamma$ cm^{-2} s^{-1} sr^{-1}) and the combined estimated instrumental background and isotropic diffuse radiation for *COS B* ($\sim 3 \times 10^{-5}\ \gamma$ cm^{-2} s^{-1} sr^{-1}) are subtracted from the data before comparing to the model. The background subtraction for the case of *COS B* is somewhat uncertain due to its nature and magnitude. In the future, improvements in angular resolution and statistics combined with a low instrumental background as expected from the EGRET instrument on the *Gamma-Ray Observatory* will be important in obtaining a more detailed understanding of the Galaxy with the use of the calculations described here.

6. MODEL RESULTS

6.1. *Comparison with Observations*

The distribution in longitude of the Galactic diffuse gamma-ray intensity predicted by the model is shown in Figures 2*a* and 2*b*. The values used for the adjustable parameters in these plots are $X = 2.0 \times 10^{20}$ molecules cm^{-2} (K km s^{-1})$^{-1}$ and $r_0 = 2$ kpc. (See also Table 2 below.) The data points shown are measurements from the *SAS 2* and *COS B* instruments for the energy range $E > 100$ MeV. The longitudinal distribution is constructed by averaging intensities over the latitude range of $|b| \leq 10°$. The contribution of three high-energy Galactic gamma-ray sources, specifically the Crab (0531+21), Geminga (1E 0630+178, Halpern & Holt 1992), and the Vela pulsars (0833−45) are evident in the data shown in these figures, but they are not added to the diffuse model. In general, the emission agrees very well with the observations of *SAS 2* and *COS B* on a large scale. The model predicts enhanced gamma-ray emission in regions associated with the spiral arms and large concentrations of gas. Latitude profiles for six intervals of longitude are shown in Figure 3. The intervals were chosen to match those used by Hartman et al. (1979) to facilitate comparison with the *SAS 2* results, although a detailed comparison would necessitate folding the model results with the *SAS 2* point spread function. For the three intervals given in the *SAS 2* paper the qualitative comparison is good. The central 40° has the same narrow peaked character. As in the *SAS 2* data, the interval from $90° < l < 175°$ has a higher "wing" toward negative latitudes. Finally, the interval from $205° < l < 250°$ shows a similar, but more pronounced

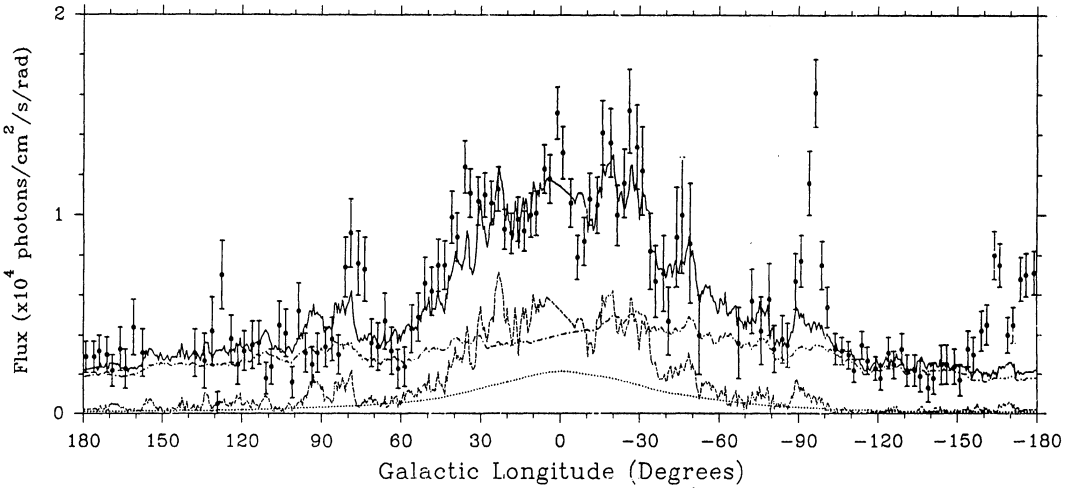

FIG. 2*a*

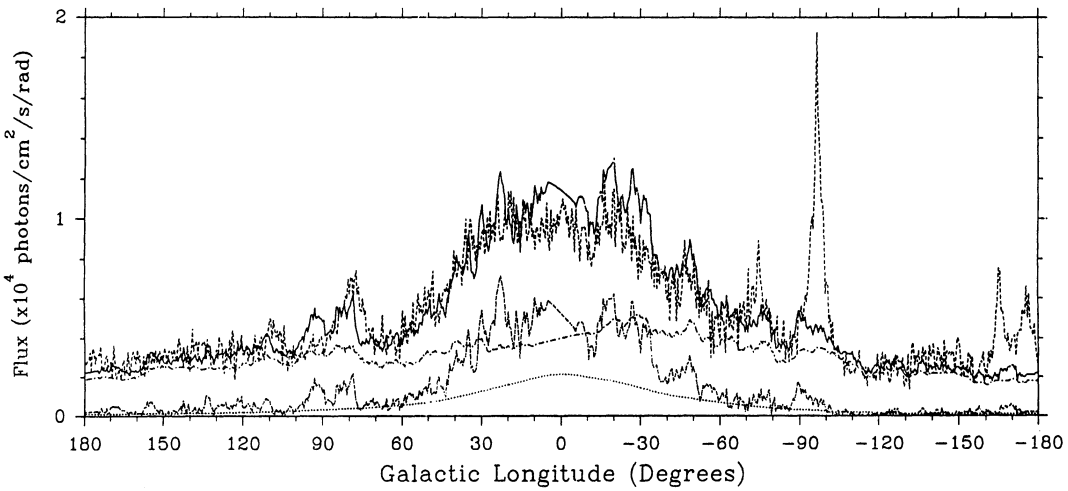

FIG. 2*b*

FIG. 2.—Gamma-ray intensity ($E > 100$ MeV) predicted by the model averaged over $|b| < 10°$ in latitude and plotted as a function of Galactic longitude. Contributions from molecular hydrogen are shown as a dash and two dots evidenced by a peak in the central 60° while contributions from atomic hydrogen are designated by a dash and one dot and are more uniform in longitude. The smooth solid line is a plot of the emission from inverse Compton interactions. The contribution from H II is shown by the dotted curve that is seen at the lowest level of all of the components. The upper solid line shows the total. (*a*) The data points correspond to *SAS 2* (Hartman et al. 1979). An extragalactic isotropic component of 4×10^{-6} photons cm^{-2} s^{-1} rad^{-1} is subtracted from the data for comparison to the model. (*b*) The uniform dashed line represents data from *COS B* (Mayer-Hasselwander et al. 1982). A constant component of 1×10^{-5} photons cm^{-2} s^{-1} rad^{-1}, corresponding to the sum of an isotropic component and estimated *COS B* instrumental background is subtracted from the data for comparison with the model. In both sets of data, the contributions from three high energy sources, as noted in the text, are evident in the data but are not included in the diffuse model.

asymmetry. The predicted intensity of the diffuse Galactic gamma radiation is shown in Figure 4 as a function of both longitude and latitude. A Gaussian smoothing function of width 0°.5 was used here. As one can see, many detailed features are predicted for comparison to data when higher resolution data exist.

Notice that by contrast in Figure 5 where the cosmic-ray density was assumed to be a constant throughout the Galaxy, there is a significant lack of gamma-ray emission from the inner Galaxy and much less variation with longitude. This result eliminates the possibility of a constant cosmic-ray distribution model unless one assumes the molecular hydrogen normalization factor X is much larger. To pursue this point, consider the distribution of molecular hydrogen within the solar circle and beyond. As discussed in § 3, much or most of the molecular gas is contained within the solar circle contrary to the more extended distribution of the atomic gas. Thus, in order to have a uniform cosmic ray distribution throughout the Galaxy consistent with the observed gamma-ray distribution, the X-factor would have to be significantly higher (by about a factor of 1.5–2) in the inner Galaxy. So far there exists no evidence for such a large negative gradient of X with Galactic radius. Quite the contrary, two recent studies suggest a positive gradient, at least beyond the solar circle, with X a factor of 2–3 higher in the outer Galaxy (Digel, Bally, & Thaddeus 1990; Sodroski 1991). However, any such increase in the outer Galaxy X-factor will not markedly affect the 2d and 3d quadrant predictions of our model since only a small fraction (see Table 1) of the Galactic molecular gas exists in that region of the Galaxy.

It is interesting to examine the prominent features in the longitude profile of gamma-ray intensity. Two of the best examples of spiral arm tangents in profiles of velocity-integrated 21 cm emission (Kerr & Kerr 1970), CO (Bronfman

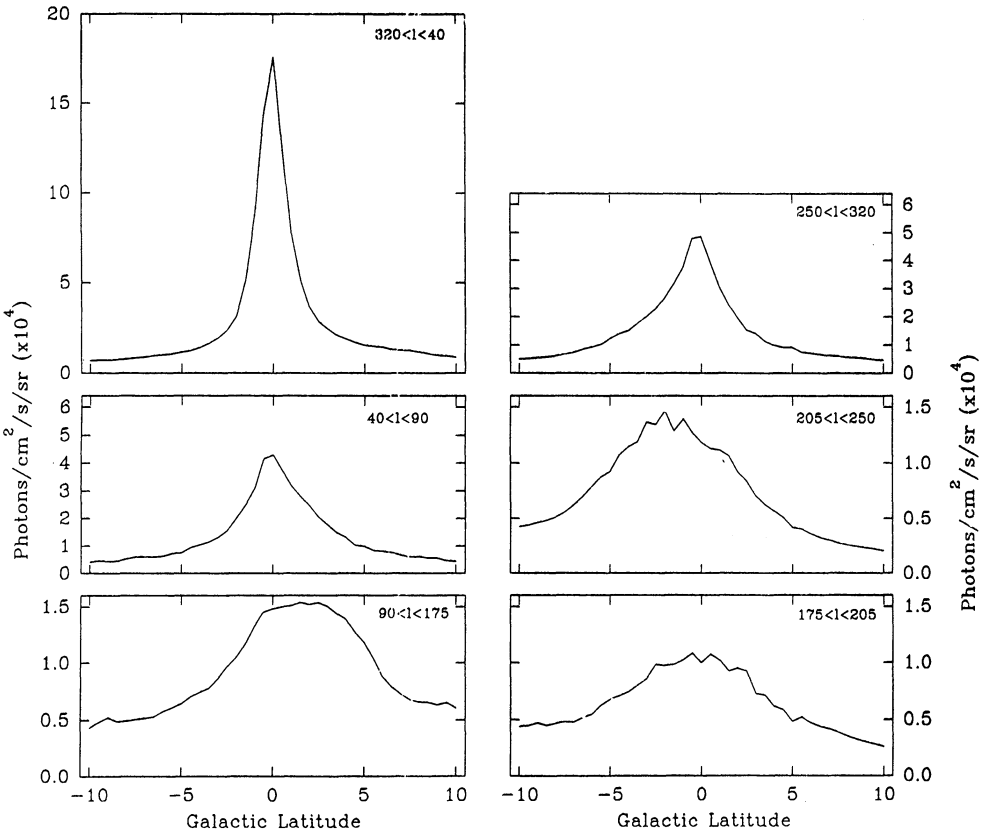

FIG. 3.—Gamma-ray intensity ($E > 100$ MeV) predicted by the model averaged over longitude intervals as a function of latitude. Three of the longitude intervals, $320° < l < 40°$, $90° < l < 175°$ and, $205° < l < 250°$, were used in the *SAS 2* analysis by Hartman et al. (1979). The other three intervals fill in the rest of the plane. As noted in the text, the model has the same characteristics as the *SAS 2* data.

et al. 1988), and radio continuum (Simonson 1970) are the Carina arm near $l = 285°$ and the Crux or Centaurus arm near $l = 315°$. Both of these are seen clearly in the *SAS 2* and *COS B* data, and their intensities are fit fairly well by the model. The other major spiral tangent in the fourth quadrant, the Norma arm near $l = 330°$, is quite apparent in the *SAS 2* data, but much less so in the *COS B* data.

It has long been known that spiral tangents are less distinct in the first quadrant than in the fourth, in part because of the geometry of trailing spiral arms, which will be more open and diverging in the fourth quadrant. The much larger amount of nearby "Great Rift" gas in the first quadrant (Dame et al. 1987) confounds the identification of tangents in existing gamma-ray surveys even further. In longitude profiles integrated over 10°–20° of Galactic latitude, such as those necessitated by the low angular resolution and counting statistics of the *SAS 2* and *COS B* surveys, the contribution of nearby clouds can be substantial. For example, the gamma-ray longitude profiles show enhanced emission toward the tangents of the Scutum ($l \approx 31°$) and 4 kpc ($l \approx 24°$) arms, but to judge from the CO data, half or more of the emission in these directions may come from the Aquila Rift, a fairly small molecular cloud lying only 200 pc away (Dame & Thaddeus 1985). Since these tangents are seen clearly in higher angular resolution tracers along the plane, however, it is possible that the higher angular resolution and sensitivity of the EGRET data will allow these tangents to be studied in detail.

The absence of a prominent peak associated with the tangent of the Sagittarius arm near $l \approx 51°$ is not surprising, since Dame et al. (1986) have shown that although the arm is well traced by molecular complexes on a large scale, few happen to lie near its tangent. The features near $l = 82°$ coincides with the very complex Cygnus X region; whether this region represents the tangent of the Local spiral arm or merely

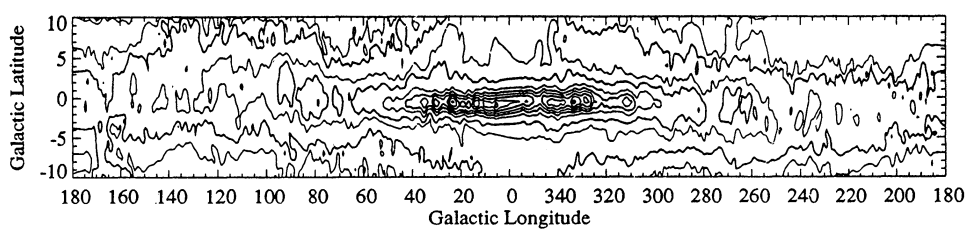

FIG. 4.—Gamma-ray intensity predicted by the model showing the distribution in Galactic coordinates. The contour values are 0.50, 0.75, 1.0, 1.5, 2.0, 3.0, 5.0, 7.0, 9.0, 12, and 19 × 10^{-4} photons ($E > 100$ MeV) cm^{-2} s^{-1} sr^{-1}. Smoothing on the scale of 1°0 has been used.

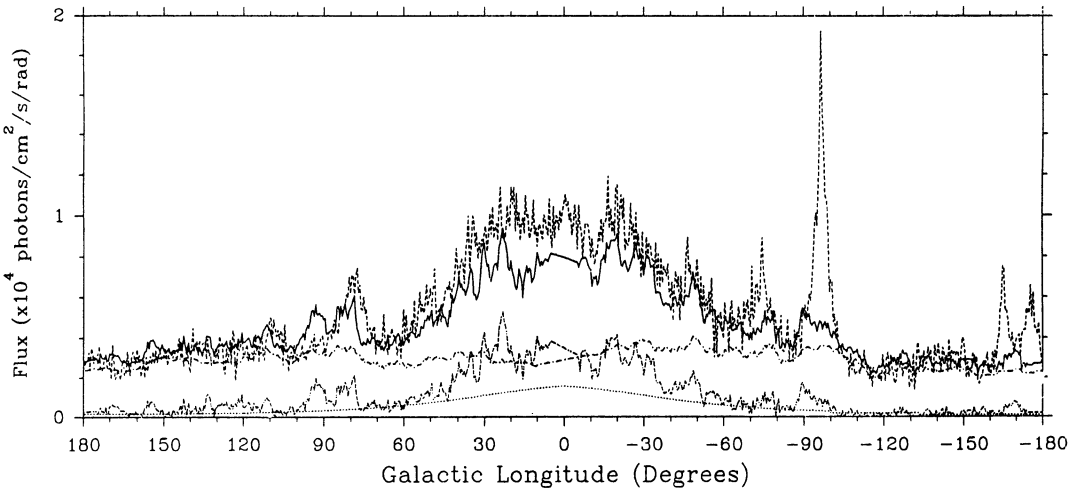

FIG. 5.—Gamma-ray intensity ($E > 100$ MeV) predicted by a constant uniform cosmic-ray density (equal to local solar value) model averaged over $|b| < 10°$ in latitude and plotted as a function of Galactic longitude. The curves of the model are the same as those used in Fig. 2. The uniform dashed line shows the *COS B* data (see Fig. 2 caption) for comparison. In this case the model prediction in the central longitudes is well below the observations.

the chance alignment of a few large molecular complexes is still unknown. What might be the opposite tangent of the Local arm, toward $l \approx 270°$, is masked in the gamma-ray profiles by the strong point source in Vela.

Perhaps as important as the prominent peaks associated with spiral arm tangents are the corresponding minima between the arms. Two classic interarm regions known to be deficient in both atomic and molecular gas are seen clearly in the gamma-ray profiles, and both are well reproduced by the model. One lies between the Sagittarius arm and Cygnus X ($l \approx 60°$–$70°$), and the other between the Vela region and the anticenter ($l \approx 210°$–$260°$).

Another feature of interest in the predicted gamma-ray emission is the latitude distribution of the radiation along the plane. Because the radiation from the central region of the Galaxy is relatively far away, the distribution is predicted to be much narrower than that from the rest of the Galactic plane. Although this effect was seen by *SAS 2* (Hartman et al. 1979) and *COS B* (Mayer-Hasselwander et al. 1982), the angular resolution of these two instruments did not permit seeing the full extent of the difference. The intensity in the narrow region is actually quite large compared to that elsewhere. This effect is not seen strongly in Figures 2*a* and 2*b* because of the averaging over a wide latitude range ($\pm 10°$). However, Figure 6 does show the strength of this effect. Future high-energy gamma-ray measurements with improved angular resolution could look for this effect. The sharpness would verify that the radiation is more distant, and the intensity measurements would assist in determining the degree of coupling of the cosmic radiation and matter. The existing gamma-ray observations do not permit a good determination of the coupling constant between the cosmic rays and the matter, but values in the range 2–3 kpc are suggested. When data of higher resolution and better statistical significance are available, the sharpness and magnitude of the contrast along the tangents to spiral arms will be important new information in this regard.

6.2. *Sensitivity of Model to Parameter Variations*

Table 2 summarizes the parameters used in the calculation. Among the seven listed there, five are quite well determined, and are not regarded as being adjustable. The first two entries, as has been discussed, are the only two that can be varied when fitting observations. The sensitivity of the model to the choices of these values is an important question when fitting data is

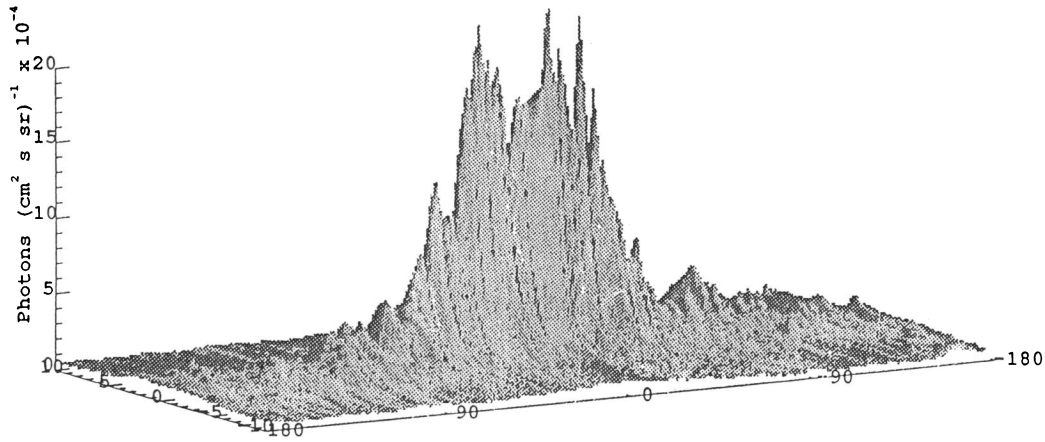

FIG. 6.—Three-dimensional representation of predicted Galactic gamma-ray diffuse radiation

TABLE 2

MODEL PARAMETERS

Parameter	Symbol	Value
CO to H_2 Conversion	X^a	(2 to 3) $\times 10^{20}$ molecules cm^{-2} (K km s^{-1})$^{-1}$
Matter, cosmic-ray coupling scale	r_0^a	2 kpc
21 cm line to H I conversion	...	1.83×10^{18} atoms cm^{-2} (K km s^{-1})$^{-1}$
Near-far matter distribution	...	Weighted by Gaussian amplitude[b]
H_2 scale height	Z_{H2}	60 pc
H I scale height	Z_{HI}	110 pc in inner Galaxy, eq. (15) in outer Galaxy
Local matter density	...	0.66 atom cm^{-3}
Galactic radius	R_{max}	20 kpc

[a] Quantities that are adjustable in the model.
[b] See text, § 5.1.

attempted. Conversely, the sensitivity to each of the parameters is useful in understanding the importance of the various assumptions of the model and on how well the adjustable parameters might be determined with the improved future observations. For these reasons, a systematic study was made of the first six quantities in Table 2; the two that are variable, and four others. First, the calculated emission was averaged over a region $\pm 10°$ in latitude from the plane and over each 30° longitude bin along the plane. Then one of the parameters was varied by 20% above its nominal value, and for each bin, the ratio to the nominal case was computed. The process was repeated for a 20% decrease. The results are shown in Figure 7 for each quantity.

It can be seen in Figure 7 that the variable parameter for the conversion from the CO measurement to molecular hydrogen (X-factor) has a strong effect on the emission in the central 120° of the plane and that the maximum effect is slightly offset into the first quadrant. On the other hand, the region of the anticenter is quite insensitive to the X-value. Likewise, the second variable parameter, the cosmic-ray smoothing scale size r_0 has similar effects, but its change is small at the 20% variation level. These parameters therefore can be adjusted to fit the center-anticenter contrast. Conversely, the model when fitted to observations gives a sensitive measure of the CO to molecular hydrogen factor in the Galactic center region. Based on the present data from *SAS 2* and *COS B* as noted above, the best choices of these two quantities are $X = 2.0 \times 10^{20}$ molecules cm^{-2} (K km s^{-1})$^{-1}$ and $r_0 = 2.0$ kpc. The improved resolution, energy range and statistics expected from EGRET promises to refine these conclusions. Moreover, even though the longitudinal variation in the averages for the two main parameters is similar, finer scale details, e.g., in the vicinity of the edges of the arm features along with the EGRET data could resolve the contributions of the two effects.

As to the other parameters, a variation in the conversion from antenna temperature to H I column density has a rela-

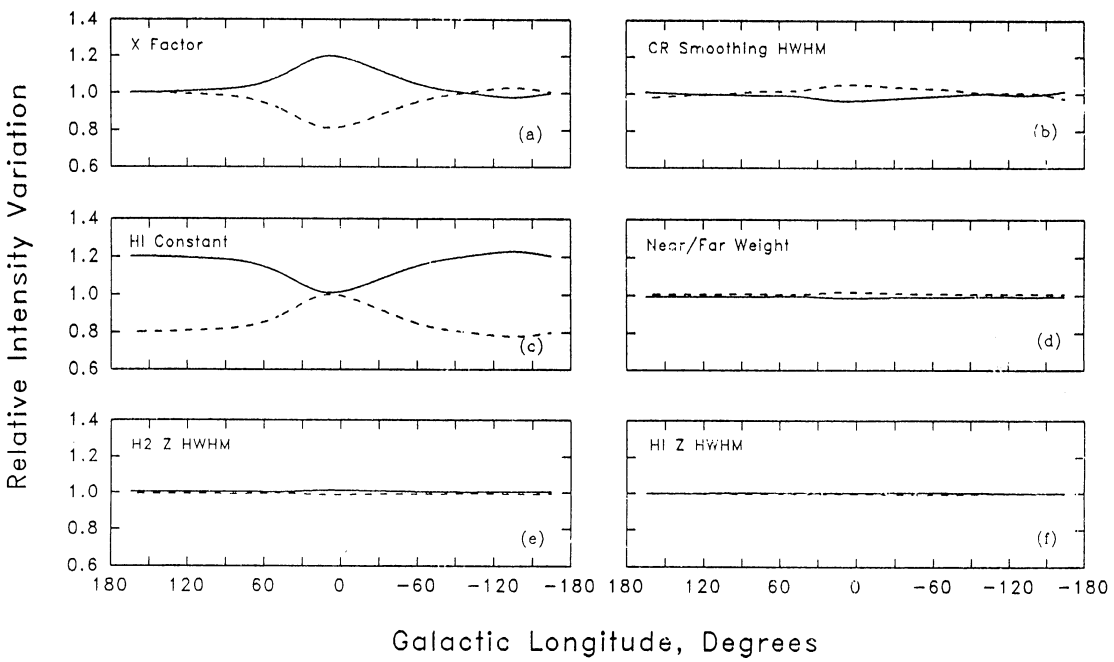

FIG. 7.—Relative intensity variation of the diffuse gamma-ray emission as a function of Galactic longitude for a variation of +20% (*solid curves*) and −20% (*dotted curves*) for the two model parameters shown in panels (*a*) and (*b*), and for the four other better established parameters. The parameters are (*a*) the conversion from the integrated CO line intensity to the molecular hydrogen column density; (*b*) the scale length of the cosmic-ray density coupling to matter; (*c*) the conversion between the 21 cm line intensity and the atomic hydrogen column density; (*d*) the weighting used to divide matter between the near and far points in the rotation curve solution of position in the inner Galaxy; (*e*) the molecular hydrogen scale height normal to the plane; and (*f*) the corresponding atomic hydrogen scale height.

tively significant effect, but only in the anticenter regions. This is because H I is dominant there. All of the other quantities have only minor variations across the full range of longitude. Notice in particular that the model results are insensitive to the assumptions about the near-far-weighting where distance ambiguity exists from the rotation curve.

7. SUMMARY

The model for diffuse emission in the Galaxy presented here incorporates recent data on the distribution of Galactic atomic and molecular hydrogen into a three-dimensional spatial array. Using known interaction cross sections and a cosmic-ray density distribution based on well-accepted concepts of equipartition and dynamic balance, it has been shown that the diffuse gamma-ray emission is remarkably consistent in magnitude and structure in the longitudinal variation with existing data. Unlike most models in the past, no multiparameter fits are required to adjust the results. Two quantities that are not firmly established have been treated as free, and approximate values were indicated (see Table 2) based on present knowledge of the Galactic diffuse intensity. Future observations can be expected to further refine their values.

The model will also serve to provide a diffuse background model to the EGRET analysis system that evaluates point sources. To this end, the output of the model is written into a standard FITS (Flexible Image Transform System) sky maps. These maps will facilitate studies of both the Galactic and extragalactic diffuse emission in the EGRET program.

REFERENCES

Bhat, C. L., Issa, M. R., Houston, B. P., Mayer, C. J., & Wolfendale, A. W. 1985, Nature, 314, 511
Bierman, L., & Davis, L. 1960, Z. Astrophys., 51, 19
Bignami, G. F., & Fichtel, C. E. 1974, ApJ, L65
Bignami, G. F., Fichtel, C. E., Kniffen, D. A., & Thompson, D. J. 1975, ApJ, 199, 54
Bloemen, J. B. G. M. 1989, ARA&A, 29, 469
Bloemen, J. B. G. M., Blitz, L., & Hermsen, W. 1984, ApJ, 279, 136
Bloemen, J. B. G. M., et al. 1986, A&A, 154, 25
Bloemen, J. B. G. M., Reich, P., Reich, W., & Schlickeiser, R. 1988, A&A, 204, 88
Bronfman, L., Cohen, R. S., Alvarez, H., May, J., & Thaddeus, P. 1988, ApJ, 324, 248
Burton, W. B. 1985, A&AS, 62, 365
———. 1988, in Galactic and Extragalactic Radio Astronomy, 2d ed., ed. G. L. Verschuur & K. Kellermann (New York: Springer), 295
Burton, W. B., & Gordon, M. A. 1978, A&A, 63, 7
Burton, W. B., & Liszt, H. S. 1983, A&AS, 52, 63
Carvallo, G., & Gould, R. J. 1971, Nuov. Cimento, 2B, 77
Casoli, F. 1991, in IAU Symp. 146, Dynamics of Galaxies and Molecular Cloud Distributions, ed. F. Combes & F. Casoli (Dordrecht: Reidel), 51
Chi, X., & Wolfendale, A. W. 1991, J. Phys. G., 17, 987
Clemens, D. P. 1985, ApJ, 295, 422
Clemens, D. P., et al. 1988, ApJ, 327, 139
Cox, P., Krügel, E., & Mezger, P. G. 1986, A&A, 155, 380
Dame, T. M., Elmegreen, B. G., Cohen, R. S., & Thaddeus, P. 1986, ApJ, 305, 892
Dame, T. M., & Thaddeus, P. 1985, ApJ, 297, 751
Dame, T. M., et al. 1987, ApJ, 322, 706
Dermer, C. D. 1986, A&A, 157, 223
Dickey, J. M., & Lockman, F. J. 1990, ARA&A, 28, 215
Digel, S., Bally, J., & Thaddeus, P. 1990, ApJ, 357, L29
Dodds, D., Strong, A. W., & Wolfendale, A. W. 1975, MNRAS, 171, 596
Fich, M., Blitz, L., & Stark, A. A. 1989, ApJ, 342, 272
Fichtel, C. E. 1989, Nucl. Physics B. (Proc. Suppl.) 10B, 3
Fichtel, C., Hartman, R., Kniffen, D., & Sommer, M. 1972, ApJ, 171, 31
Fichtel, C., Hartman, R., Kniffen, D., Thompson, D., Bignami, G., Ögelman, H., Özel, M., & Tümer, T. 1975, ApJ, 198, 163
Fichtel, C. E., & Kniffen, D. A. 1984, A&A, 134, 13
Fichtel, C. E., Özel, M. E., Stone, R. G., & Sreekumar, P. 1991, ApJ, 374, 134
Fichtel, C. E., Simpson, G. A., & Thompson, D. J. 1978, ApJ, 222, 833
Fichtel, C. E., & Trombka, J. I. 1981, Gamma-Ray Astrophysics, New Insights into the Universe (NASA SP-453)
Fuchs, B., Schlickeiser, R., & Thielheim, K. O. 1976, ApJ, 206, 589
Georgelin, Y. M., & Georgelin, Y. P. 1976, A&A, 49, 57
Ginzburg, V. L., & Syrovatskii, S. I. 1964, The Origin of Cosmic Rays (Oxford: Pergamon)
Grabelsky, D. A., Cohen, R. S., Bronfman, L., & Thaddeus, P. 1988, ApJ, 331, 181
Halpern, J. P., & Holt, S. S. 1992, Nature, 357, 222
Harding, A. K., & Stecker, F. W. 1985, ApJ, 291, 471
Hartman, R., Kniffen, D., Thompson, D., & Fichtel, C. 1979, ApJ, 230, 597
Henderson, A. P., Jackson, P. D., & Kerr, F. J. 1982, ApJ, 263, 116
Kerr, F. J., Bowers, P. F., Jackson, P. D., & Kerr, M. 1986, A&AS, 66, 373
Kerr, F. J., & Kerr, M. 1970, Astrophys. Lett., 6, 175
Kerr, F. J., & Lynden-Bell, D. 1986, MNRAS, 221, 1023
Kniffen, D., Hartman, R., Thompson, D., & Fichtel, C. 1973, ApJ, 186, L105
Koch, H. W., & Motz, J. W. 1959, Rev. Mod. Phys., 31, 920
Kraushaar, W., Clark, G., Garmire, G., Borken, R., Higbie, P., Leong, V., & Thorsos, T. 1972, ApJ, 177, 341
Kulkarni, S. R., Blitz, L., & Heiles, C. 1982, ApJ, 259, L63
Kulkarni, S. R., & Heiles, C. 1988, in Galactic and Extragalactic Radio Astronomy, 2d ed., ed. G. L. Verschuur & K. Kellermann (New York: Springer), 95
Kutner, M. L., & Leung, C. M. 1985, ApJ, 291, 188
Lebrun, F., et al. 1983, ApJ, 274, 231
Lockman, F. J. 1984, ApJ, 283, 90
Maloney, P., & Black, J. H. 1988, ApJ, 325, 389
Mathis, J. S., Mezger, P. G., & Panagla, N. 1983, A&A, 128, 212
Mayer-Hasselwander, H. A. 1985, Explanatory Supplement to the *COS B* Data Base (available from K. Bennett, Space Science Dept., ESTEC, Noordwijk, The Netherlands)
Mayer-Hasselwander, H., et al. 1980, Ann. NY Acad. of Sci. No. 336, Ninth Texas Symposium on Relativistic Astrophysics (Munich), 211
———. 1982, A&A, 105, 164
Mihalas, D., & Binney, J. 1981, Galactic Astronomy: Structure and Kinematics, 2d ed. (San Francisco: Freeman)
Parker, E. N. 1966, ApJ, 145, 811
———. 1968, Stars and Stellar Systems VII, Nebulae and Interstellar Matter, ed. B. M. Middlehurst & L. H. Aller (Chicago: Univ. Chicago Press), 707
———. 1969, Space Sci. Rev., 9, 654
———. 1977, Cosmic Ray Propagation and Containment, in The Structure and Content of the Galaxy and Galactic Gamma Rays (NASA CP-002)
Paul, J., Casse, M., & Cesarsky, C. J. 1975, Proc. 14th Internat. Cosmic-Ray Conference (Munich), 1, 59
Puget, J. L., Ryter, C., Serra, G., & Bignami, G. 1976, A&A, 50, 247
Reich, P., & Reich, W. 1988, A&A, 196, 211
Schlickeiser, R., & Thielheim, K. O. 1974a, Phys. Letters, 53B, 369
———. 1974b, A&A, 34, 109
Scoville, N. Z., & Solomon, P. M. 1975, ApJ, 199, L105
Shull, J. M., & Van Steenberg, M. E. 1985, ApJ, 294, 599
Simonson, S. C. 1970, A&A, 9, 163
Sodroski, T. J. 1991, ApJ, 366, 95
Solomon, P. M., & Barrett, J. W. 1991, in IAU Symp. 146, Dynamics of Galaxies and Molecular Cloud Distributions, ed. F. Combes & F. Casoli (Dordrecht: Reidel), 235
Solomon, P. M., & Rivolo, A. R. 1989, ApJ, 339, 919
Stark, A. A., Gammie, C. F., Wilson, R. W., Bally, J., Linke, R. A., Heiles, C., & Hurwitz, M. 1992, ApJS, 79, 77
Stecker, F. W. 1970, Ap&SS, 6, 377
———. 1979, ApJ, 228, 919
———. 1988, in Cosmic Gamma Rays, Neutrinos and Related Astrophysics, ed. M. M. Shapiro & J. P. Wefel (Dordrecht: Reidel) 85
Stecker, F. W., Solomon, P. M., Scoville, N. Z., & Ryter, C. E. 1975, ApJ, 201, 90
Strong, A. W., et al. 1987, Proc. 20th Internat. Cosmic Ray Conf. (Moscow) OG 2.2-6
———. 1988, A&A, 207, 1
Taylor, J. H., & Cordes, J. M. 1993, ApJ, 411, 674
Thielheim, K. O. 1975, in Origin of Cosmic Rays, ed. J. L. Osborne & A. W. Wolfendale (Dordrecht: Reidel), 165
Thielheim, K. O., & Langhoff, W. 1968, J. Phys. A., Ser. 2, 1, 694
Thompson, D. J., & Fichtel, C. E. 1982, A&A, 109, 352
Thompson, D., Fichtel, C., Hartman, R., Kniffen, D., & Lamb, R. 1977, ApJ, 213, 252
Weaver, H. F., & Williams, D. R. W. 1973, A&AS, 8, 1
Wouterloot, J. G. A., Brand, J., Burton, W. B., & Kwee, K. K. 1990, A&A, 230, 21